Structural and optical study of amorphous hydrogenated silicon nitride thin film as antireflection coating on solar cell

Swati Mamgain[*]

Nanotech Laboratory, Department of Physics, Indian Institute of Technology Delhi, Delhi 110016, India

[*]Corresponding author: Tel: (+91)9819522821; E-mail: smswati583@gmail.com

Abstract

The structural, optical and electrical aspects of as deposited as well as annealed amorphous hydrogenated silicon nitride (a-SiN$_x$: H) thin films of different stoichiometry, grown on silicon wafer by radio frequency- plasma enhanced chemical vapor deposition (RF-PECVD) are thoroughly investigated. Photoluminescence (PL) measurement verify that Si rich a-SiN$_x$: H (SRSN) film of refractive index 2.68, gives good PL as compared to near stoichiometric film and support the presence of Silicon quantum dots (Si QDs) embedded in a-SiN$_x$: H matrix. Detailed structural analysis by high resolution transmission electron microscopy (HRTEM) revealed that as deposited SRSN thin film contains amorphous Silicon quantum dots (a-Si QDs) which are grown by phase separation of SRSN film during the synthesis process. These SRSN thin films of different thicknesses have been deposited at the surface of Silicon solar cell as anti-reflection coatings (ARCs). By reflectance measurement, it is observed that the ARC contains a-Si QDs in a-SiN$_x$: H matrix, more effectively minimize the reflection of incident light across the wavelengths ranging from 300 to 800 nm. With a-Si QDs/ a-SiN$_x$: H ARC, we demonstrate an increase in short circuit current density, open circuit voltage and conversion efficiency by 4.34 mA/cm^2, 0.01V and 0.21% (absolute) respectively and indicate its utility in improving the performance of Si solar cells. Copyright © 2017 VBRI Press.

Keywords: Solar cell, quantum dots, reflectance, antireflection coating, efficiency.

Introduction

For solar cells, one of approaches for improving their efficiency is to decrease the reflection of the incident light by the modification of front surface. As far as this, various arrangements have been suggested to achieve this purpose, like antireflection coatings (ARCs) [1, 2], surface Passivation and texturizations [3, 4] etc. Lots of reports are available regarding the antireflection coatings on solar cells. Generally, Silicon nitride (SiN$_X$) layers are mostly used as ARCs on solar cells [5]. Ideally, this coating not only reduces the reflection of incident light but together provides good surface and bulk passivation. Usually hydrogen is used to passivate grain boundaries and bulk defects. All these requirements are fulfilled by silicon nitride fabricated at low temperature 200^{0}C - 450^{0}C by using PECVD method [6-7]. B. Liu and co-workers observed a low optical reflection with silicon nitride double-layer coating [8]. Recently, Singh HK *et al.* have showed a minimization in reflection using ultra-thin film of silver, sandwiched between silicon nitride ARC layers on c-Si substrate [9]. From last few years, significant efforts have been done to get enhanced light absorption in silicon solar cells by applying nanostructures like quantum dots (QDs), nano wires etc. [10]. It has been found that the metal nanoparticles patterned on a dielectric layer and embedded in it [11, 12] or directly onto a substrate [13, 14] reduce the reflection of incident light over a broad spectral range.

Gold or silver nanoparticle arrays, on top of the front surface of solar cells, reveal the low and uniform reflectance curve across the broad wavelength range (400 nm -1100 nm) due to their surface plasmon excitation effect [15]. Similarly, Semiconducting and Insulating nanostructures also provide a highly effective light absorption, if dense (spacing ~500 nm) and high-aspect-ratio nanostructure-arrays are used as ARC in the front of solar cell [16]. Recently, P. Spinelli *et al* used a periodic array of cylindrical Si nanoparticles (Si NPs) on a Si$_3$N$_4$ layer. Experimental results and Simulations revealed a 2% lower reflectance over the wavelength range of 450 – 900 nm [17].

The intention of the present research is to investigate the structural, optical, electrical aspects of PECVD deposited a-SiN$_x$: H thin films as ARC by varying concentration of Silicon and the effect of post deposition annealing on these films. In this work, we also present a study of front surface modification for Si solar cells by combining a-SiN$_x$:

H layer with a-Si QDs (a-Si QDs are embedded in a-SiN$_x$: H layer) as antireflection coating, to realise a minimization in reflection of incident light across the wavelengths ranging from 300 to 800 nm. We observed enhanced cell performance, i.e., an increase in open circuit voltage (V_{oc}), short circuit current density (J_{sc}) and efficiency by using a-Si QDs/ a-SiN$_x$: H as antireflection coating on Silicon solar cell.

Experimental

Materials

a-SiN$_x$:H thin films of different stoichiometry, named as S1 and S2 have been deposited on p-type Silicon (100) wafer and on quartz substrate, by RF-PECVD (PECVD: Samco Model PD-2S) deposition system. This system uses RF (13.56MHz) power to maintain glow discharge and produce ionized species necessary for the growth of thin film. Here Argon-diluted silane (4 % SiH$_4$ in 99.99 % pure Ar) and ammonia (99.998 % pure NH$_3$) have been used as precursor gases. During deposition the flow rate of SiH$_4$, SiH$_4$ partial pressure, chamber pressure, plasma power, deposition temperature and deposition time have been fixed at 80 sccm, 0.32 mbar, 1.1 mbar, 25 W, 200°C and 2 min respectively for all the films. NH$_3$ partial pressure for S1 & S2 has been fixed at 0.06 mbar and 0.02 mbar respectively. After deposition, both samples have been subjected to thermal annealing at 700^{0}C and 800^{0}C by using a quartz tube furnace with an ambient gas N$_2$ (99.995 % pure) + 5% H$_2$ (99.99 % pure) over 30 min.

Methods

Refractive index measurements were carried out with the help of Gaertener Ellipsometer, in which a He-Ne laser (632.8nm) beam with 1mm spot diameter is used as a light source. To obtain refractive index (n), ellipsometric angles; delta (Δ) and psi (Ψ) were fitted by using a spline model. X-ray reflectivity (XRR) carried out in X-ray diffractometer (Bruker D8 Discover) using Cu K$_\alpha$ (λ = 0.154 nm) radiation to determine the thickness and density of as deposited as well as of annealed film. Photoluminescence (PL) measurements were taken out by using 337 nm nitrogen lasers (pulse frequency 200Hz, JSC Plasma) as an excitation source at Room-temperature (RT). PL of these two set of samples gave us clue about the presence of QDs, so for verification of it, high resolution transmission electron microscopy (HRTEM: Technai G2) was carried out at operating voltage of 200 kV. Ultraviolet/visible (UV-Vis) spectroscopy (UV3600: Shimazdu) was carried out to determine the reflectance of SRSN thin films deposited on Si substrate as well as on Si solar cell. For efficiency calculation, Photo current measurements were done with the help of solar simulator (Newport Corporation, USA) under AM1.5G illumination.

Results and discussion

Refractive index has been measured 2.2 and 2.68 for sample S1 and S2 respectively. The refractive index of a-Si is 3.44 and with increase of nitrogen contents the

refractive index decreases monotonically to approach the refractive index of stoichiometric amorphous silicon nitride, which is approximately 1.85 at 633 nm wavelength [18]. It shows that the sample S2 is more silicon rich than sample S1.The X-Ray Reflectivity (XRR) spectra of S1 and S2 as deposited, as well as annealed samples are shown in **Fig. 1.**
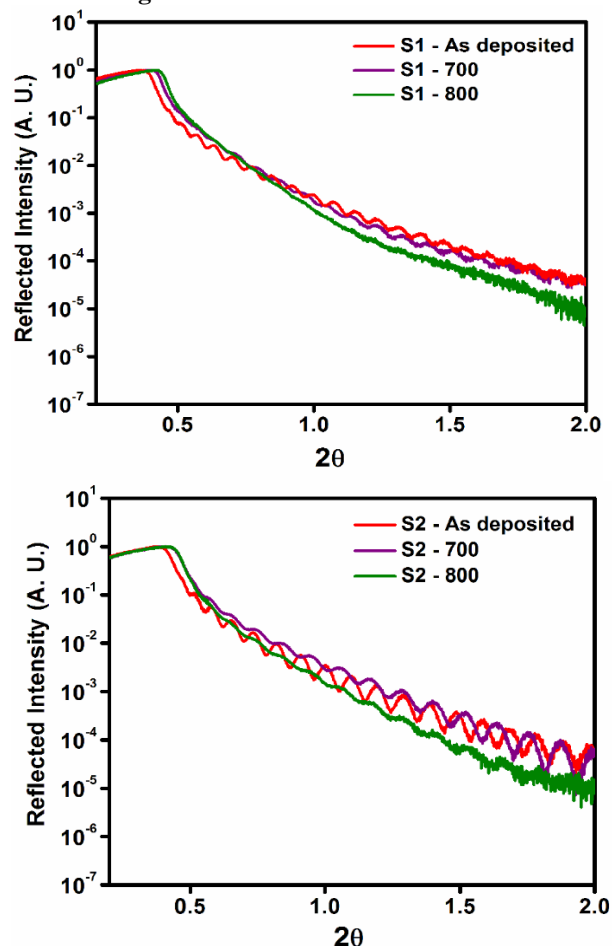

Fig. 1. XRR spectra of S1 and S2 as deposited as well as annealed

Table. 1. Thickness and Densities of S1, S2 set of samples

Sample	Critical Angle	Thickness (nm)	Density (gm/cc)
S1 As deposited	0.192	95.6	1.722
S1 Annealed at 700^0 **C** (S1 - 700)	0.206	83	1.982
S1 Annealed at 800^0 **C** (S1 - 800)	0.210	83	2.059
S2 As deposited	0.199	78	1.849
S2 Annealed at 700^0 **C** (S2 - 700)	0.213	66	2.119
S2 Annealed at 800^0 **C** (S2 - 800)	0.217	64	2.199

Table 2. Solar cell performance parameters.

Sample	V_{oc} (V)	I_{sc} (A)	J_{sc} (mA/cm^2)	Fill factor	Efficiency
With a-Si QDs/ a-SiN$_x$: H ARC	0.51	0.019	31.21	0.66	10.69%
With standard Si$_3$N$_4$ ARC	0.52	0.039	35.55	0.59	10.90%

It has been observed that, due to the removal of hydrogen from the samples, both films (S1 and S2) became more compact and thinner after annealing. At the same time, as annealing temp. is increased, there is more decrease in thickness and increase in density of films as more voids inside the films have been removed at a higher annealing temperature.

Fig. 2 shows the Room temperature PL measurements of sample S1 and S2, at excitation wavelength of 337 nm. It has been observed that PL is not symmetric enough. So it is not fitted by a single Gaussian peak instead fitted by three peaks; red, green, and blue. The PL from these samples has been reported to be broadly composed of contributions from radiative defects, Band tail recombination and a-Si QDs [19]. Various defects, such as silicon dangling bonds (Si-DBs), nitrogen dangling bonds (N-DBs) exist in the band gap of silicon nitride. These defect states can involve the radiative recombination of electrons and holes in silicon nitride, and playing a role as luminescent centers [19, 20]. Here the red peak is corresponding to a-Si QDs centered at the energies of 2.1 (±) eV. Green peak is corresponding to Si-DBs centered at the energies of 2.4 eV. The third blue peak is corresponding to N-DBs centered at the energies of ~3.0eV respectively [19].
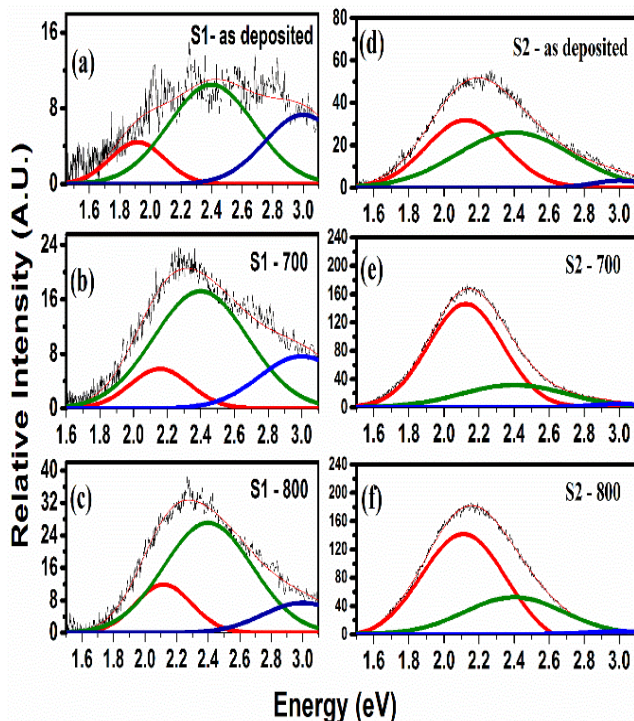
In case of both set of samples, after annealing there is increase in PL intensity. It has been observed that the component of PL which might be due to a-Si QDs (corresponding to red peak), increased very well after annealing. This increase in intensity is more definite in case of sample S2. Since S2 is more silicon rich, so there is more probability of diffusion of Si to the nucleation sites and this can lead to the formation of a-Si QDs. In this way PL of these samples gave us clue about the presence of QDs and so for verification, HRTEM carried out. **Fig. 3** shows the HRTEM image of as deposited S2 sample. In this image, black Patches represent a-Si QDs which might be grown by phase separation of SRSN during the synthesis process. In this image black Patches represents the quantum dots. Thus the PECVD deposited SRSN film exhibiting PL in visible region is also possible material for down-conversion in Si solar cells.
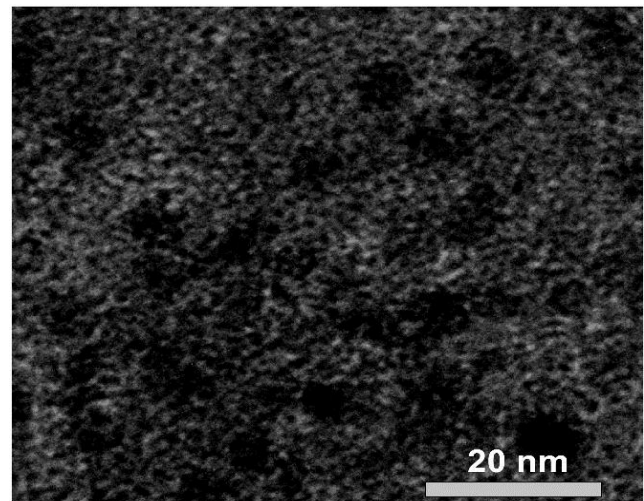

Fig. 3. HRTEM image of as deposited S2 sample.

Fig. 2. PL Spectrum of S1 and S2 (as deposited, as well as annealed samples) at excitation wavelength of 337 nm.
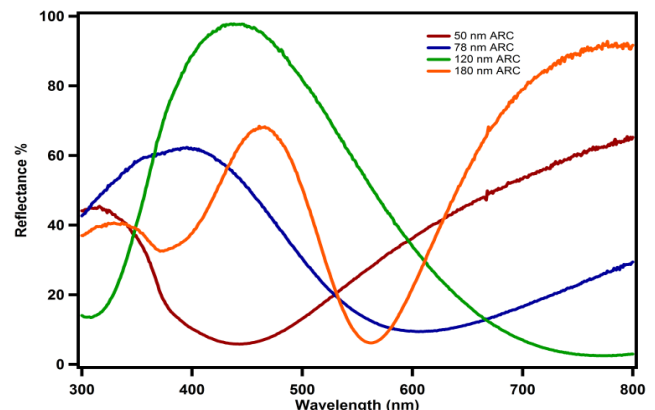

Fig. 4. Reflectance of a-SiN$_x$: H thin films coated on Si substrate.

For solar cell application, SRSN film with deposition parameters (except deposition time) corresponding to S2 has been chosen as ARC. To study the optical reflection, SRSN films of different thicknesses (50 nm, 78 nm, 120 nm and 180 nm) were coated on Si substrate as well as on the surface of commercial Si solar cell. Reflectance spectrum of these films was recorded across the wavelengths ranging from 300 to 800 nm as shown in **Fig. 4** (Reflectance of SRSN films coated on Si substrate) and **Fig. 5** (Reflectance of SRSN films coated on the surface of commercial Si solar cell)**.**

Solar cell reflectance with different thickness ARCs clearly indicate that in visible region all of them (except solar cell with 180 nm ARC) show a huge reduction in reflectance. It has been seen that Si solar cell with 78 nm ARC which contains a-Si QDs embedded in the matrix of a-SiN$_x$: H, shows a lowest and constant dip in reflectance. The strong reduction of reflectance can be explained by the mutual effect of the preferred forward scattering of the incident light from a- Si QDs and the destructive interference from a-SiN$_x$: H layer **[17]**. Applying the 78 nm thick a-Si QDs/ a-SiN$_x$: H ARC to a crystalline Si solar cell improves power conversion efficiency under AM1.5G illumination by 0.21% with respect to reference cell (Cell with 80-nm-thick standard silicon nitride ARC) (**Fig. 6**).

This enhancement in cell performance may be attributed to the less reflection of incident light and photoluminescence through down-shifter mechanism of a-Si QDs. a- Si QDs convert photons with higher energy into lower energy in the form of PL, which are absorbed more proficiently by Si solar cell **[21]**. This is for the first time in this work; SRSN films not only work as antireflection coating but also work as luminescence down converter, due to the presence of a-Si QDs. But the increase in efficiency is somewhat lesser than the expected one. One of the possible reasons is the charge recombination. So, further study is needed for complete understanding.

Conclusion

SRSN films of different stoichiometry were deposited with RF-PECVD system by varying SiH$_4$ / NH$_3$ gas ratio. In addition, deposited films were subjected to thermal annealing at 700^{0}C and 800^{0}C in N$_2$ + 5% H$_2$ ambient. A strong visible PL at RT has been observed for all the films. The PL is mainly due to the presence of a- Si QDs and defect states (Si-DBs, N-DBs) within the band gap of silicon nitride. The presence of a-QDs has been verified by HRTEM measurement and shows that the a-Si QDs are embedded in the matrix of silicon nitride. As a solar cell application, 78 nm ARC (contains a-Si QDs embedded in the matrix of a-SiN$_x$: H) shows a lowest and constant dip in reflectance because of the combined effect of preferred forward scattering of incident light from a- Si QDs and the destructive interference from a-SiN$_x$: H layer. A power conversion efficiency enhancement of 0.21 % was observed in Si solar cell with a-Si QDs/ a-SiN$_x$ film as an ARC layer compared to a reference cell. This enhancement in efficiency may be attributed to the less

reflection of incident light and photoluminescence through down-shifter mechanism of a-Si QDs. The new ARC concept suggested in this work offers a useful efficiency improvement in silicon solar cells.
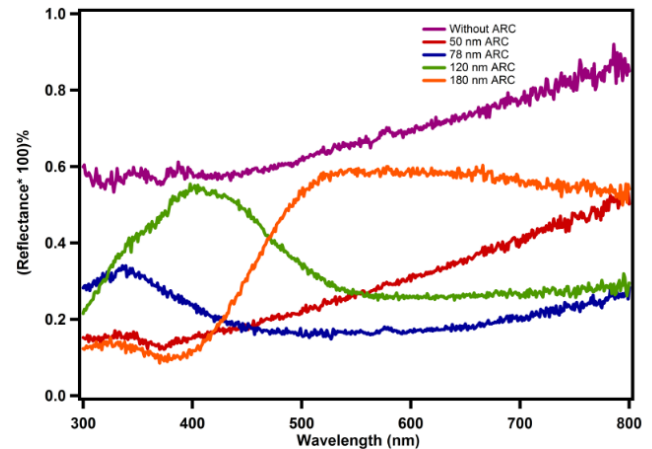

Fig. 5. Reflectance of Si solar cell with a-SiN$_x$: H thin films as antireflection coating.
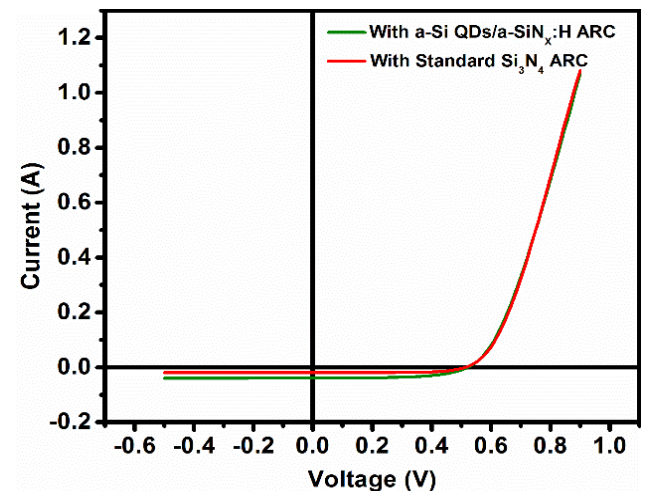

Fig. 6. Current–Voltage (*I–V*) Characteristics of Si solar cell with a- Si QDs/ a-SiN$_x$:H ARC and standard Si$_3$N$_4$ ARC.

References

1. Chhajed, S.; Schubert, M. F.; Kim, J. K.; Schubert, E. F.; *Appl. Phys. Lett.*, **2008**, *93*, 251108.
   DOI: 10.1063/1.3050463
2. Hocinea, D.; Belkaida, M. S.; Pasquinellib, M.; Escoubasb, L.; Simonb, J. J.; Rivièreb, G. A.; Moussic A.; *Mater. Sci. Semicond. Process.* , **2013**, *16*, 113.
   DOI: 10.1016/j.mssp.2012.06.004
3. Han, K. S.; Shin J. H.; Lee, H.; *Sol. Energy Mater. Sol. Cells.*, **2010**, *94*, 583.
   DOI: 10.1016/j.solmat.2009.12.001
4. Ulbrich, C.; Gerber, A.; Hermans, K.; Lambertz, A.; Rau, U.; *Prog. Photovolt: Res. Appl.*, **2013**, *21*, 1672.
   DOI: 10.1002/pip.2249

5. Iwahashi, T.; Morishima, M.; Fujibayashi, T.; Yang, R.; Lin, J.; Matsunaga, D.; *J. Appl. Phys.,* **2015**, *118*, 145302.
   DOI: 10.1063/1.4932639
6. Aberle, A. G.; *Sol. Energy Mater. Sol. Cells*., **2001**, *65*, 239.
   DOI: 10.1016/S0927-0248(00)00099-4
7. Lamers, M.; Hintzsche, L. E.; Butler, K. T.; Vullum, P. E.; Fang, C. M.; Marsman, M.; Jordan, G.; Harding, J. H.; Kresse, G.; Weeber, A.; *Sol. Energy Mater. Sol. Cells*., **2014**, *120*, 311
   DOI: 10.1016/j.solmat.2013.04.026
8. Liu, B.; Qiu, S.; Chen, N.; Du, G.; Sun, J.; *Mater. Sci. Semicond. Process*., **2013**, *16,* 1014.
   DOI: 10.1016/j.mssp.2013.02.019
9. Singh, H. K.; Sharma, P.; Solanki, C. S.; *Plasmonics,* **2014**, *9*, 1409.
   DOI: 10.1007/s11468-014-9757-5
10. Behzad Esfandiarpour; Integration of Nanostructures and Quantum Dots into Spherical Silicon Solar Cells; University of Waterloo, **2013**.
11. Branham, M. S.; Chun Hsu, W.; Yerci, S.; Loomis, J.; Boriskina, S.V.; Hoard, B. R.; Han, S. E.; Chen G.; *Adv. Mater.,* **2015**, *27*, 2182.
    DOI: 10.1002/adma.201405511
12. Brongersma, M. L.; Cui, Y.; Fan, S.; *Nat. Mater*., **2014**, *13*, 451.
    DOI: 10.1038/NMAT3921
13. Rahman, A.; Ashraf, A.; Xin, H.; Tong, X.; Sutter, P.; Eisaman, M. D.; Black, C. T.; *Nat. Commun*., **2015**, *6*, 5963.
    DOI: 10.1038/ncomms6963
14. Wang, B.; Leu, P. W.; *Nano Energy,* **2015**, *13*, 226.
    DOI: 10.1016/j.nanoen.2014.10.040
15. Wang, Z.; Sun, C.; Wang, X.; *Plasmonics*, **2016**, 1, 8.
    DOI: 10.1007/s11468-016-0302-6
16. Han, S. E.; Chen, G.; *Nano Lett*., **2010**, *10*, 1012.
    DOI: 10.1021/nl904187m
17. Spinelli, P.; Verschuuren, M. A.; Polman, A.; *Nat. Commun*., **2012**, *3*, 692.
    DOI: 10.1038/ncomms1691
18. Hong, J.; Kessels, W. M. M.; Soppe, W. J.; Weber, A. W.; Arnodbik, W. M.; van de Sanden, M. W. M.*; J. Vac. Sci. Technol. B,* **2003***, 21,* 2123.
    DOI: 10.1116/1.1609481
19. Bommali, R. K.; Singh, S. P.; Rai, S.; Mishra, P.; Sekhar, B. R.; *J. Appl. Phys*., **2012**, *112*, 123518.
    DOI: 10.1063/1.4770375
20. Wang, M.; Li, D.; Yuan, Z.; Yang, D.; Que, D.; *Appl. Phys. Lett*. **2007**, *90*, 131903.
    DOI: 10.1063/1.2717014
21. Trupke, T.; Green, M. A.; Würfel, P.; *J. Appl. Phys*. **2002**, *92*, 1668.
    DOI: 10.1063/1.1492021